Rare-earth site distributions in R(PO$_3$)$_3$ (R = La, Nd, Er, Yb) metaphosphate glasses by Reverse Monte Carlo simulations

U. Hoppe

Rostock University, Institute of Physics, Rostock D-18051, Germany

The R–R pair distribution functions of rare-earth metaphosphate glasses R(PO$_3$)$_3$ with R = La, Nd, Er, Yb are determined from total X-ray and neutron scattering data by the Reverse Monte Carlo method. Characteristic features of the resulting pair distribution functions $g_{RR}(r)$ are small peaks at ~0.44 nm followed by great broad peaks at ~0.63 and ~0.85 nm and a smooth feature at ~1.1 nm. With the decrease of the radii of the R^{3+} ions by ~0.023 nm if R is changed from La to Yb the peaks of the R–R distances shift to smaller lengths. Accordingly, the features in the $S_{RR}(Q)$ factors shift to greater Q-values except for the first diffraction peaks which appear at constant position of ~12 nm^{-1}. The decrease of the area of the peak at ~0.44 nm with decreasing R radii is interpreted with decreasing fractions of O atoms in terminal P–O bonds which possess two R first-neighbours. The resulting $g_{RR}(r)$ functions are modelled with structures based on the monoclinic Yb(PO$_3$)$_3$ crystal. The characteristics of the series of $g_{RR}(r)$ and $S_{RR}(Q)$ functions give support to the $g_{\mathrm{TbTb}}(r)$ and $S_{\mathrm{TbTb}}(Q)$ data reported for a magnetic difference neutron diffraction experiment on Tb meta-phosphate glass.
PACS: 61.10.Nz, 61.12.Ld, 61.43.Bn, 61.43.Gt

1. Introduction

Investigations of the medium-range order (MRO) of oxide glasses possess still challenging character. The determination of the distribution of the network-modifying ions in host glass matrices is main part of this work. Knowledge of the structural arrangement of the metal ions is useful to understand definite glass properties. For example, the nearest-neighbour distances between the rare-earth sites in rare-earth doped oxide glasses play a great role for the luminescence and magnetic properties of the corresponding materials [1].

Diffraction experiments are suitable to extract MRO information, thus, the structural information of atomic distances which exceed lengths of ~0.4 nm. But the use of diffraction experiments for clarifying the MRO deals with several problems: Only pair distance information on the level of the sample average is determined which is expressed by means of probability functions. The binary rare-earth phosphate glasses $(R_2O_3)_x$ $(P_2O_5)_{1-x}$ whose R site distributions are subject of this paper possess three different atomic species. Consequently, six independent pair distribution functions $g_{ij}(r)$ merge into the total $g(r)$ function obtained from a single diffraction experiment. Several contrast variation techniques are capable to extract partial $g_{ij}(r)$ functions. Some methods have already been used to determine the R–R correlations of binary rare-earth phosphate glasses. A first great distance peak in the $g_{RR}(r)$ function at ~0.56 nm indicating 7.9 neighbours was found by neutron diffraction (ND) with isomorphic substitution of Dy by Ho [2,3]. The Tb–Tb correlations of a Tb metaphosphate glass $(x \cong 0.25)$ were extracted by the magnetic scattering fraction of neutrons scattered on the paramagnetic Tb sites [4]. Tb–Tb distances of ~0.6 nm were estimated from the position of the first scattering peak in the $S_{\mathrm{TbTb}}(Q)$ structure factor. Q is the modulus of the scattering vector with $Q = (4\pi/\lambda)\sin\theta$ where λ is the radiation wavelength and 2θ is the scattering angle. Recently, another magnetic difference neutron diffraction experiment was performed on the Tb metaphosphate glass, as well, where it was possible to obtain the $g_{\mathrm{TbTb}}(r)$ function from the $S_{\mathrm{TbTb}}(Q)$ data by Fourier transformation [5]. Tb–Tb distance peaks were found at ~0.39, ~0.64 and ~0.85 nm. The anomalous change of the neutron scattering length of Sm was used to extract the Sm–Sm correlations in neutron diffraction experiments of a

Sm phosphate glass ($x \cong 0.20$) [6]. The $g_{SmSm}(r)$ function of this ultraphosphate glass ($x < 0.25$) clearly differs from the $g_{TbTb}(r)$ function of the Tb metaphosphate glass [5] indicating the dependence of the MRO on the R_2O_3 content. The contrast variation techniques mentioned are difficult. The structural information of interest is contained in a small fraction of the total neutron scattering data and, thus, its extraction is sensitive to experimental and correction problems.

On the other hand, the rare-earth ions are comparably strong scatterer in X-ray diffraction (XRD) experiments. As shown in Table 1, a distance between a pair of R atoms possesses clearly more weight than any other pair distance. Differently, P–O and O–O distances possess most weight in total ND data. Thus, the use of the information of the R–R correlations existing in XRD data can help to obtain reliable $g_{RR}(r)$ functions. The Reverse Monte Carlo (RMC) method [7] is suitable to extract the $S_{RR}(Q)$ factors from the total XRD intensities if reasonable constraints for the other pair distributions improve the reliability of the approach. The RMC simulations of the structures of Eu and Tb metaphosphate glasses by Mountjoy et al. [8] were performed using the XRD data only. More promising in the RMC approach is the combination of XRD and ND data which we already used in an earlier investigation of the structure of the La metaphosphate glass [9].

Different from neutron diffraction, the conditions of XRD experiments on R(PO$_3$)$_3$ glasses, i.e., the scattering power and absorption of the R atoms, change little and monotonously if the R species is changed. Thus, XRD is highly suitable to study those structural effects in the $g_{RR}(r)$ functions which are caused by decreasing ionic radii with increase of the electron numbers of the R species. The R–O distances decrease by ~0.023 nm and the R–O coordination numbers decrease from ~7 to ~6 if R is changed from La to Yb [10-12]. RMC will be used to determine the R–R correlations for a series of R(PO$_3$)$_3$ glasses with selected R changing from La to Yb. The earlier RMC runs [9] of the La(PO$_3$)$_3$ glass are repeated using better XRD data [13] which are obtained at a synchrotron beamline with high-energy photons. Other ND data [12,14] of R(PO$_3$)$_3$ glasses with R = Nd, Y, Yb are available for RMC and are used together with the XRD data [12] obtained with high-energy synchrotron radiation. The structures of R(PO$_3$)$_3$ glasses with R = Er and Y are assumed to be almost identical according to R–O and R–P first-neighbour distances found to be equal each other, respectively [12].

2. Reverse Monte Carlo simulations

The Reverse Monte Carlo method is used to extract the $g_{RR}(r)$ functions from results of two independent experiments, XRD and ND. Three independent sets of experimental scattering data of different contrast of the R sites are needed for unequivocal determinations of the $g_{RR}(r)$ functions, e.g., by the isomorphic subst-itution technique [2,3]. Other constraints in our RMC approach such as minimum separation distances and coordination numbers are used to compensate for the deficit of information. Moreover, the underlying three-dimensional atomic configurations are a good check for the physical reliability of the experimental scattering data. Different variants of the combination of scattering data and the other constraints exist. Here, criterion for the successive improvement of the atomic configurations in the cubic boxes with periodic boundary condi-tions is the agreement between the experimental and calculated structure factors, $S_k(Q)$. Thus, RMC is used as a fit of the experimental $S_k(Q)$ data using the Monte Carlo technique by minimization of a value χ^2 which is calculated with

$$\chi^2 = \Sigma_{k,l}\left[S_{k,\exp}(Q_l) - S_{k,\mathrm{mod}}(Q_l)\right]^2 \quad . \tag{1}$$

k denotes the XRD and ND data by X and N and l indicates the measuring points. A new position of an arbitrarily chosen atom is accepted with $\chi_m^2 < \chi_{m-1}^2$ in every case where $m-1$ denotes the move of atoms accepted just before. The probability $p = \exp\left[-\left(\chi_m^2 - \chi_0^2\right)/s\right]$ determines which of the unfavourable moves

are accepted, as well. χ_0^2 is calculated for the initial configuration. Value s has a similar effect as the temperature factor. The RMC code used [9,15] differs from that of McGreevy & Pusztai [7] in the handling of the coordination constraints. Maximum coordination numbers, N_{ij}, can be defined for the individual sites but the instantaneous N_{ij}'s do not effect the calculation of parameter χ^2.

Number densities of atoms, ρ_0, varying from 66 to 68 nm^{-3} were calculated from mass densities measured for the $R(PO_3)_3$ glasses with R = La, Nd, Y, Yb [9,12,14]. For simplicity, the small variations of ρ_0 or R_2O_3 contents and the small contaminations with crucible material [12] are neglected in the RMC simulations. Values ρ_0 of 67 nm^{-3} and R_2O_3 contents of 25 mole% are used. 3900 atoms, among them 300 R atoms, fill the cubic model boxes with edge lengths of 3.88 nm.

The scattering data used for the different samples do not possess identical quality. Unlike Q-ranges (Q_{max} of 223 or 280 nm^{-1}) were realized in different XRD runs [12-14] on the BW5 beamline of the synchrotron DORIS III (Hamburg/Germany). Also the Q-ranges of the ND runs on different instruments at ISIS (Chilton/ UK) vary with Q_{max} of 500 nm^{-1} (LAD; R = La) [9], 250 nm^{-1} (SANDALS; Nd) [14] and 280 nm^{-1} (GEM; Y, Yb) [12]. Accordingly, the upper limits Q_{max} of the $S_X(Q)$ and $S_N(Q)$ factors used in RMC differ with 223 and 470 nm^{-1} for R = La, 223 and 250 nm^{-1} for R = Nd and 280 nm^{-1} for the other $S(Q)$ factors, respectively. The RMC runs for the Er(PO$_3$)$_3$ glass make use of the $S_X(Q)$ data of Er(PO$_3$)$_3$ glass and the $S_N(Q)$ of Y(PO$_3$)$_3$ glass. For better comparability with the other three glasses modelled by RMC, the additional information of the $S_X(Q)$ factor of the Y(PO$_3$)$_3$ glass is not used in the RMC runs but it is compared subsequently.

According to the knowledge of experimental results of $R(PO_3)_3$ metaphosphate glasses [9-14] the glass structure is formed of PO$_4$ tetrahedra with oxygen atoms on the tetrahedral corners and the P atoms in the centre. Numerous spectroscopic studies as reviewed [16] have shown that these PO$_4$ units are connected with others via two corners for glasses of $x = {\sim}0.25$. This behaviour implies the existence of infinite chains and/or ring structures formed of the PO$_4$ units where the R^{3+} ions occupy interstitial voids. Experimental methods for determination of the chain lengths or fractions of ring structures for the materials studied are not known. The structures of related crystals, the orthorhombic La(PO$_3$)$_3$ and monoclinic Yb(PO$_3$)$_3$ polyphosphates [17,18], are formed of infinite chains of PO$_4$ tetrahedra where the La^{3+} ions in La(PO$_3$)$_3$ possess eight, the Yb^{3+} in Yb(PO$_3$)$_3$ possess six oxygen neighbours. Oxygen atoms in the P–O–P bridges (O$_B$) are not first-neighbours of R^{3+} ions but every oxygen atom (terminal O$_T$) with one P neighbour coordinates one or two R^{3+} sites. Constraints in accordance with these features are introduced to obtain reasonable atomic configurations: (I) PO$_n$ units with $n > 4$ are suppressed. (II) Oxygen atoms coordinate two P neighbours in maximum. (III) The PO$_4$ units are allowed to form links through two corners to be arranged in long chains and/or rings and are not allowed to share edges. (IV) Finally, minimum separation distances, $L\min_{ij}$, of the different pairs of atoms are defined and shown in Table 2. These parameters are introduced to suppress unreasonable short-range structures. The Lm_{ij} values are chosen smaller than the known lengths of the short-range order of the same glasses [12] and the related crystal structures [17,18]. The first-neighbour distances in acceptable RMC results are determined by pair distributions from scattering data etc. but not by Lm_{ij} parameters. The Lm_{RP} and Lm_{RO} lengths (Table 2) decrease with decreasing R–O distances. The Lm_{RR} lengths were also varied in first RMC runs starting with 0.43 nm for R = La. But these values were reduced to constant 0.37 nm to avoid any R-dependent effects and to allow for R–R distances of 0.39 nm which are known of the

LaP$_3$O$_9$ crystal [17]. Essential changes of the $g_{RR}(r)$ functions after this decrease of Lm_{RR} were not observed.

The initial atomic configurations are taken from the earlier RMC work of the La(PO$_3$)$_3$ glass [9]. Some artefacts of the model structures such as PO$_3$ groups (~5%) are minor defects which fraction could not be reduced further. The final functions are averages of ten atomic configurations which were obtained in intervals of $>10^5$ accepted moves of single atoms. The experimental structure factors used in the RMC runs are well approximated with the model functions calculated from the final atomic configurations (cf. Fig. 1). Also the model $S_X(Q)$ function for R = Er agrees with the experimental XRD data of the Y(PO$_3$)$_3$ glass. This $S_X(Q)$ factor was not used in the RMC runs but the model function is calculated from those RMC configurations which were obtained by the $S_N(Q)$ factor of Y(PO$_3$)$_3$ glass and the $S_X(Q)$ factor of Er(PO$_3$)$_3$ glass. The assumption of identical structures for Y(PO$_3$)$_3$ and Er(PO$_3$)$_3$ glasses is justified.

The definitions of the functions used are given shortly before the results extracted from the RMC configurations are presented: The partial radial distribution functions $RDF_{ij}(r)$ change if atoms of species i or j are moved. Accordingly, the corresponding partial $S_{ij}(Q)$ factors are calculated in each step of RMC by fast Fourier transformation with

$$S_{ij}(Q) = 1 + \int_0^{r_{\max}} \left[RDF_{ij}(r)/r - 4\pi r c_i \rho_0 \right] \sin(Q r) \, dr \ . \tag{2}$$

It is assumed that significant correlations do not exist for distances greater than $r_{\max}$ ($r_{\max}$ = 1.6 nm is used). c_i is the mole fraction of atomic species i. The model $S_X(Q)$ and $S_N(Q)$ factors are calculated from the $S_{ij}(Q)$ factors for determination of the current χ^2-values.

The resulting $RDF_{RR}(r)$ functions of the final RMC configurations are used to determine the R–R coordination numbers and mean separation lengths of the distance peaks. For illustration of the peaks it is more convenient to show correlation functions $T_{ij}(r)$ or pair distribution functions $g_{ij}(r)$ which are defined with

$$T_{ij}(r) = RDF_{ij}(r)/r = 4\pi r g_{ij}(r) c_i \rho_0 \ . \tag{3}$$

These functions increase only linearly or are constant in the limit of great distances. If considering the $T_{ij}(r)$ or $g_{ij}(r)$ functions it is remembered that relations between the peak areas are not equivalent to relations between the numbers of atomic neighbours.

3. Results

The contribution of the $S_{RR}(Q)$ factor to the total $S_X(Q)$ data is illustrated before the final series of R–R correlations for the four different R is shown. The weighted partial $w_{ij}(Q) \cdot S_{ij}(Q)$ functions which compose the total $S_X(Q)$ factor of the La(PO$_3$)$_3$ glass (on top of Fig. 1) are shown in Fig. 2a. The weighting factors $w_{ij}(Q)$ are given with $w_{ij}(Q) = (2 - \delta_{ij}) c_i c_j f_i(Q) f_j(Q) / < f >^2$ in Faber-Ziman notation [19] where $< f >$ is the compositional average of the $f_i(Q)$ atomic scattering amplitudes (polynomial approximation of Waasmaier & Kirfel [20]). δ_{ij} is the Kronecker symbol which is unity in case of $i = j$, otherwise zero. Though the La atoms are strong scatterer for X-rays the corresponding $w_{LaLa}(Q)$ factors are small with 11% for $Q = 0$ due to the small La fraction of 1/13 (14% for $w_{YbYb}(Q)$). Nevertheless, the partial $w_{LaLa}(Q) \cdot S_{LaLa}(Q)$ factor is

the main contribution to the shoulder at ~12 nm^{-1} in the $S_X(Q)$ factor. Also the $S_{PP}(Q)$, $S_{PO}(Q)$ and $S_{OO}(Q)$ factors contribute to this peak while the $S_{LaP}(Q)$ and $S_{LaO}(Q)$ factors show minima at this position. Obviously, the P and O sites produce the same character of MRO as the La sites do. The P and O atoms surround the network holes occupied by the La^{3+} ions and, thus, accentuate the MRO of the La sites. The oscillations following the first peak in the $S_{LaLa}(Q)$ factor are small and of small periods. Stronger oscillations occur in the $S_{LaP}(Q)$, $S_{LaO}(Q)$ and $S_{PO}(Q)$ factors even for greater Q. They exhibit longer periods due to the narrow La–P, La–O and P–O first-neighbour peaks which exist in the corresponding pair distributions (Fig. 2b). The La–La pair distribution function $g_{LaLa}(r)$ is comparably smooth. It is noisy due to small La fractions existing in the model configurations. Three La–La distance peaks are identified at ~0.47, ~0.65 and ~0.87 nm which are followed by a smooth feature at ~1.1 nm.

The $S_{LaLa}(Q)$ and $g_{LaLa}(r)$ functions are found similar to those of all rare-earth metaphosphate glasses studied. The peaks in the $g_{RR}(r)$ functions shift to smaller lengths with decreasing radius of the R^{3+} ions (Fig. 3) which is a reasonable behaviour. The area of the peak at ~0.44 nm decreases, as well, which change is due to a decrease of R–O coordination numbers, N_{RO} [10-12]. The N_{RO} values of the R(PO$_3$)$_3$ metaphosphate glasses of the greater R^{3+} ions in the lanthanide series are significantly greater than six [9-14]. But only six O$_T$ are available to coordinate an R^{3+} ion [21,22]. Assuming that O$_B$ do not participate in the coordination of the R sites the R^{3+} ions have to share some O$_T$ neighbours and R–R distances of ~0.44 nm attributable to R–O$_T$–R linkages occur. The peak at ~0.44 nm appears very small for the Yb(PO$_3$)$_3$ glass. It should vanish completely in case of $N_{RO} = 6$. The distances of ~0.63 nm were attributed to separations between two R^{3+} ions which coordinate different O$_T$ sites of a common PO$_4$ neighbour [5,13]. This interpretation is not exact: The number of Yb neighbours at these distances is eight in the Yb(PO$_3$)$_3$ crystal [18] but only six of these Yb are connected with the central Yb site via the edge of a PO$_4$ tetrahedron. The distance peak at ~0.85 nm belongs to R sites which are separated by two or more PO$_4$ units. The numbers of R neighbours and the mean distances belonging to the peaks at ~0.44, ~0.63 and ~0.85 nm are determined and shown in Table 3. Estimated uncertainties of N_{RRm} and r_{RRm} are given where the arbitrariness in choosing the limits $r_{max\,m}$ (minima between the peaks), the use of $x = 0.25$ instead of exact compositions and systematic error of experimental structure factors (normalization deficits etc.) are taken into account. The distances as well as the numbers of R neighbours belonging to each R–R peak decrease with decreasing R–O separations. Both tendencies would change the packing densities in opposite direction but here they compensate each other and maintain constant packing densities such as found for the metaphosphate glasses of the different R species [12].

Fig. 4 shows the $S_{RR}(Q)$ factors belonging to the $g_{RR}(r)$ functions given in Fig. 3. The functions change uniformly with decreasing R–O distances, as well. The features in the range $Q > 20\,nm^{-1}$ shift continuously to greater Q as expected for shorter R–R distances if R is changed from La to Yb. On the other hand, the first diffraction peaks in the $S_{RR}(Q)$ data do not follow this shift but they appear at constant positions of ~12 nm^{-1}.

Before the functions $g_{RR}(r)$ and $S_{RR}(Q)$ presented in Figs. 3 and 4 are discussed it is noticed that the RMC configurations do not accomplish the expectations in all details: Fractions of ~5% of the P atoms have only three oxygen neighbours. Accordingly, the lengths of the chains formed of corner-connected PO$_4$ groups possess only finite size while infinite chains and/or cyclic structures are expected [16-18]. The oxygen sites with different numbers of neighbours illustrate the problem. Table 4 compares the fractions of these oxygen

sites (O$_T$, O$_B$) possessing different numbers of R neighbours for crystal structures and RMC models. The values of the Yb(PO$_3$)$_3$ crystal [18] with $N_{RO} = 6$ show that all O$_T$ possess one R neighbour and all O$_B$ atoms do not coordinate R sites. Since O$_T$ are not shared between R neighbours R–R pairs of short distances (N_{RR1}) do not exist. For the La(PO$_3$)$_3$ crystal [17] with $N_{RO} = 8$ one third of the O$_T$ (fraction O$_{T,2}$) is shared by R–R pairs which leads to some short R–R distances ($N_{RR1} = 2$). A mixed structure (m7) with $N_{RO} = 7$ is added to illustrate that increasing fractions of O$_{T,2}$ and N_{RR1} are due to the increase of N_{RO} according to $N_{RR1} = N_{RO} - 6$. Actually, a value N_{RR1} of 0.4 is obtained for the Yb(PO$_3$)$_3$ glass where a value of 0.5 is calculated according to the N_{YbO} of 6.5. A value N_{RR1} of 1.3 is obtained for the La(PO$_3$)$_3$ glass which is close to 0.9 as calculated for N_{LaO} of 6.9.

Table 4 shows that the values N_{RO} found in the RMC models are little less than those obtained from peak fitting [12]. The total fractions of the O$_T$ and O$_B$ sites are close to those expected at metaphosphate composition and found in the related crystal structures [17,18]. The expected oxygen sites O$_{T,1}$ and O$_{B,0}$ dominate the RMC configurations. But some unreasonable details appear: Unfavourable O$_{T,0}$ and O$_{B,1}$ sites exist while the fraction of expected O$_{T,2}$ is comparably small. This behaviour contradicts with the needs of local charge compensation. For example, sharing of an oxygen by one P and two R sites (O$_{T,2}$) is more probable than sharing by two P and one R sites (O$_{B,1}$). Thus, a significant density of defects exists in the RMC models of the R(PO$_3$)$_3$ glasses. The structural behaviour of the individual atoms is not well constrained in the diffraction data and the corresponding details of the RMC models are not useful for further analysis. Results closer to the expected behaviour were obtained by Molecular Dynamics (MD) simulations of Tb metaphosphate glass [23]. All O neighbours of the Tb^{3+} ions are O$_T$ sites. The local order of atoms in MD models seems better constrained due to the effects of the pair potentials. Nevertheless, main features of metaphosphate glasses (chains of two-fold corner-connected PO$_4$ units which coordinate R^{3+} ions by their two O$_T$ corners) are reproduced in our RMC models. Accordingly, the corresponding six pair correlations are supposed to reflect the main structural characteristics of R(PO$_3$)$_3$ glasses which justifies further discussion of the resulting $g_{RR}(r)$ functions. Support to this interpretation comes from inspecting the total $T_X(r)$ functions [12] of the glasses studied (Fig. 5): The peaks at ~0.65 and ~0.85 nm are at similar positions to peaks in the $g_{RR}(r)$ functions (Fig. 3, Table 3). But direct separation of these R–R peaks from the total $T_X(r)$ data is not possible. Determinations of lengths and coordination numbers by peak fitting were made for the P–O, R–O and O–O first-neighbours [12]. The separation of overlapping R–O and O–O peaks was possible due to the change of contrast of $T_X(r)$ and $T_N(r)$ data. For even visible P–P and strong R–P peaks (Fig. 5) only rough estimations of the coordination numbers can be given [12]. The problem is due to overlaps with unknown P–O and O–O second-neighbour correlations. The first R–R peak at ~0.44 nm interferes with R–O second-neighbour correlations.

4. Discussion

In a comparison of our $g_{RR}(r)$ and $S_{RR}(Q)$ functions with those mentioned in the Introduction best agreement reveals with the behaviour of the $g_{TbTb}(r)$ and $S_{TbTb}(Q)$ data from magnetic difference neutron diffraction [5] if it is assumed that the Tb–Tb correlations can be interpolated from the Nd–Nd and Er–Er correlations here presented. The ratio of Tb neighbours for the Tb–Tb peaks at 0.39 and 0.64 nm was reported with ~0.07 [5]. The corresponding ratios of our RMC models of the R(PO$_3$)$_3$ glasses range from 0.05 to 0.16 for R = Yb and La, respectively (Table 3). The distances r_{RR1} from RMC (~0.44 nm) are little greater than the smallest Tb–Tb separation reported in [5] (0.39 nm). This difference can be attributed to uncertain

definitions of $r_{max\,1}$ (Table 3) and the effects of R–O second-neighbour distances of similar lengths. A third peak at ~0.85 nm was also found in the reported Tb–Tb correlations [5] but the number of the corresponding neighbours is not given [5]. The experimental results for the Tb metaphosphate glass [5] and the RMC work here presented are confirmed by the findings of an MD simulation [23] where also Tb–Tb neighbours are detected at ~0.4 nm in front of a broad peak at ~0.6 nm. The peak at ~0.4 nm is attributable to separations between Tb sites which coordinate a common O_T neighbour. Unfortunately, the MD work [23] does not report any Tb–Tb coordination numbers and information on the third Tb–Tb peak is missing.

Sequences of peak positions are useful to differentiate if rare-earth sites are arranged at random or if they possess a special order. From the length ratio $\sqrt{3}$ of the first two Ca–Ca distances of ~0.38 and ~0.65 nm Gaskell et al. [24] concluded a crystal-like order of the Ca sites in Ca metasilicate glass. Since the R–R peak at ~0.4 nm is a small effect which is nearly negligible for the $Yb(PO_3)_3$ glass the peaks following this distance have to be considered in comparisons of different MRO models. In earlier work [9,12], we used a simple approach for the R site distributions in rare-earth metaphosphate glasses: R-centred spheres were assumed to be arranged in the sense of a close-packed random order. Blétry [25] used this model for the MRO of simple network glasses. The model of spheres is applicable if all R environments possess equal properties, i.e. if equal distances exist to the first R neighbours in arbitrary direction from a given R site. This behaviour is possible at metaphosphate composition with $N_{RO} = 6$: each PO_4 unit connects two R sites via its two O_T [16]. The R-centred spheres are thought to be formed of R^{3+} ions with a shell of PO_4 units belonging half to the one and to the other R neighbour. The diameter of spheres is less than twice the R–P distance because a partial interpenetration of spheres is possible. The small effect of O_T possessing two R neighbours is neglected. The position Q_1 of the first peak in the $S_{RR}(Q)$ factor is related to the diameter D of the spheres with $Q_1 = \sim 2\pi / \left(\sqrt{2/3}\, D \right) = \sim 7.7 / D$. This equation is valid in a great range of packing densities [25]. Distance $\sqrt{2/3}\, D$ is known as the separation of 111-planes of a face-centred cubic (fcc)-lattice. The prominent R–R first-neighbour distance of ~0.63 nm as the distance of the closest contact is related to the position (~12 nm^{-1}) of the first maximum in $S_{RR}(Q)$ according to the given equation. The peak positions found for the RMC models of the glasses obey the relation of a close-packed random order (cf. Figs. 3 and 4).

The $g_{RR}(r)$ function of a close-packed random order of hard spheres can be modelled easily. Results of a computer-aided simulation are used with 10000 spheres in a cubic model box [26]. The number density is chosen with 5.2 nm^{-3} according to that of the R sites in the $R(PO_3)_3$ glasses. The diameters of the spheres are varied by ±10% within the frame of a triangular distribution in order to simulate soft spheres. That broadens the peak of first neighbours. The mean diameters, i.e. the packing fractions, were adjusted so that the first-neighbour peak of the model fits that at ~0.63 nm in the RMC $g_{RR}(r)$ functions. The resulting R–R correlations are compared in Fig. 6 for R = Yb and La. The model does not reproduce the peaks at ~0.44 nm which is a shortcoming for $g_{LaLa}(r)$ but negligible for $g_{YbYb}(r)$. The model peaks at ~0.63 nm are still narrow and correspond to more R neighbours than found by RMC. The first diffraction peak of the close-packed random order of spheres appears at ~12 nm^{-1} as expected [25]. But distance peaks of ~0.85 nm found by RMC are missing in the model $g_{RR}(r)$ functions from random packing. Only smooth contributions exist in this range. The subsequent smooth feature at ~1.1 nm is somehow reproduced. Similar to the results obtained for the Ca–Ca correlations in Ca metasilicate glass [24] a random packing of the modifier sites is not the appropriate model though the first prominent R–R distance at ~0.63 nm agrees with the random packing model. A small shift detected for the first feature in the total $S_X(Q)$ factors to greater Q by ~1 nm^{-1} if R is changed from La to Yb was interpreted with the decrease of R–R distances [12] according to the random

packing model. Here it is found that the first peaks in the $S_{RR}(Q)$ factors possess constant positions independent of the R species and it is suggested that the shift of the shoulder at ~12 nm^{-1} in front of the main maximum in the $S_X(Q)$ factors results from changes of the weighting factors.

The $g_{YbYb}(r)$ data from RMC are compared with those calculated from the crystal structure of Yb(PO$_3$)$_3$ [18] (Fig. 6a). The distribution of the particular Yb–Yb distances of the crystal structure is convoluted with a Gaussian function whose width is adjusted to yield a good fit of the peak at 0.61 nm. Actually, both peaks at 0.61 and 0.83 nm possess similar shape and position for the structures of the glass (RMC result) and the related crystal [18]. Clear differences exist for distances >1.0 nm where the Yb–Yb correlations of the glass are smeared out. It is difficult to identify the reason for the special MRO of the Yb sites in the glass which is similar to that of the monoclinic crystal [18]. The arrangement of Yb sites of the crystal structure can be simplified to hexagonal symmetry and the corresponding $g_{YbYb}(r)$ function gives a good agreement with the RMC result, as well (Fig. 6a). A remarkable feature is the greater number of Yb neighbours at ~0.83 nm if compared with that at ~0.61 nm (crystal and glass; cf. Table 3). It is assumed that, due to the needs of the accommodation of the (PO$_3$)$_\infty$ chains, the number of first Yb neighbours at the contact distance is limited where the greatest peak exists in case of random packing. In Chapter 3 it is mentioned that the majority of Yb neighbours at ~0.63 nm is connected to the central Yb site via the edge of a PO$_4$ tetrahedron. This behaviour limits the number of Yb neighbours at ~0.63 nm. The small number of Yb neighbours at ~0.61 nm is compensated by a second shell at a little greater distance (~0.83 nm) formed of even more Yb neighbours.

The $g_{RR}(r)$ functions (RMC) do not show great changes in character with change from Yb to La except for the intensity of the peak at ~0.44 nm. The model $g_{YbYb}(r)$ function calculated from the structure of the monoclinic Yb(PO$_3$)$_3$ crystal [18] shows also similarity with the $g_{LaLa}(r)$ data from RMC (Fig. 6b). The comparison is made with the Yb–Yb distances of the Yb(PO$_3$)$_3$ crystal [18] because atomic structures of the other known monoclinic R(PO$_3$)$_3$ forms of symmetry P2$_1$/c are not reported. The small difference of the peak positions to 0.65 and 0.87 nm is due to greater size of the La^{3+} ions. Thus, the $g_{RR}(r)$ functions of all rare-earth metaphosphate glasses show similarity with the R–R distances of the monoclinic form regardless of the size of the R^{3+} ions. The same relation was found by comparison of the X-ray scattering intensities obtained for powders of the Gd(PO$_3$)$_3$ glass and the monoclinic Gd(PO$_3$)$_3$ crystal [12]. Ilieva et al. [27] have shown that the IR spectra of the metaphosphate glasses with R = La, Pr, Nd, Gd are similar with those of the monoclinic but not the orthorhombic crystal forms. Moreover, it was found [27] that recrystallization of metaphosphate glasses with R = La, Pr, Nd, Gd, Dy, Y leads first to the monoclinic forms. These forms appear metastable for the R(PO$_3$)$_3$ of the greater R^{3+} ions with R from La to Gd where stable orthorhombic forms [17] exist. The $g_{LaLa}(r)$ function is calculated with the La–La distances of the orthorhombic La(PO$_3$)$_3$ crystal [17] and compared with the RMC result, as well. The orthorhombic form [17] shows a La–La peak at 0.42 nm due to shared O$_T$ sites which distance is little shorter than from RMC. The subsequent La–La peak at ~0.72 nm is 'out of phase' with the peaks of the RMC result and a peak at ~0.87 nm is missing. The orthorhombic La(PO$_3$)$_3$ crystal [17] shows a strange feature: the LaO$_8$ polyhedron shares an edge with a PO$_4$ unit. The O$_T$ atoms of this edge are shared with neighbouring LaO$_8$ polyhedra. This is a very special arrangement which could contribute to a glass structure only marginally.

5. Conclusions

(1) The Reverse Monte Carlo method was successfully used to extract partial $g_{RR}(r)$ and $S_{RR}(Q)$ functions of rare-earth metaphosphate glasses R(PO$_3$)$_3$ (R = La, Nd, Er, Yb) where the X-ray diffraction data are the main source of information. Uniform changes of the features in the resulting functions for R = La to Yb

confirm the reliability of the approach. The results agree well with those from magnetic difference diffraction experiments and Molecular Dynamics methods reported for Tb metaphosphate glass.

(2) The $g_{RR}(r)$ functions show three peaks at ~0.44, ~0.63 and ~0.85 nm with numbers ~1, ~7.5 and ~9 of R neighbours, respectively. The corresponding R–R coordination numbers and distances decrease slightly with decreasing size of the R^{3+} ions if R is changed from La to Yb. Accordingly, the peaks of the $S_{RR}(Q)$ shift to greater Q. Exception is the constant position of the first diffraction peak at ~12 nm^{-1}.

(3) R–R distances of ~0.44 nm are due to a small fraction of pairs of R^{3+} ions sharing oxygen neighbours in terminal P–O bonds. The tendency for sharing oxygens is weak for glasses with R = Er and Yb. The effect increases for glasses with the greater R^{3+} ions such as La^{3+} and Nd^{3+}.

(4) The positions of the prominent first distance peak at ~0.63 nm and the first diffraction peak at ~12 nm^{-1} obey the relation for a random packing of R-centred spheres. However, the second peak of R–R distances at ~0.85 nm is already not described by this simple model.

(5) The R–R distances at ~0.63 nm and ~0.85 nm are well modelled by the Yb–Yb distances of the monoclinic Yb(PO$_3$)$_3$ crystal. Obviously, constraints of the R site distributions which are inherent to this special crystalline form are also effective in the glass structures.

Acknowledgements

References

[1] Carini G, D'Angelo G, Tripodo G, Bartoletta A, Fontana A, Rossi F and Saunders G A 1998 *Philos. Mag. B* **77** 449

[2] Martin R A, Salmon P S, Fischer H E and Cuello G J 2003 *J. Phys.: Condens. Matter* **15** 8235

[3] Martin R A, Salmon P S, Fischer H E and Cuello G J 2003 *Phys. Rev. Lett.* **90** 185501

[4] Brennan T, Saunders G A, Rainford B D, Eccleston R S, Smith R I, Carini G, D'Angelo G and Tripodo G 2003 *J. Non-Cryst. Solids* **332** 60

[5] Cole J M, Hannon A C, Martin R A and Newport R J 2006 *Phys. Rev. B* **73** 104210

[6] Cole J M, Wright A C, Newport R J, Sinclair R N, Fischer H E, Cuello G J and Martin R A 2007 *J. Phys.: Condens. Matter* **19** 056002

[7] McGreevy R L and Pusztai L 1988 *Mol. Simul.* **1** 359

[8] Mountjoy G, Anderson R, Bowron D T and Newport R J 1998 *J. Non-Cryst. Solids* **232-234** 227

[9] Hoppe U, Kranold R, Stachel D, Barz A and Hannon A C 1998 *J. Non-Cryst. Solids* **232-234** 44

[10] Anderson R, Brennan T, Cole J M, Mountjoy G, Pickup D M, Newport R J and Saunders G A 1999 *J. Mater. Res.* **14** 4706

[11] Cole J M, van Eck E R H, Mountjoy G, Anderson R, Brennan T, Bushnell-Wye G, Newport R J and Saunders G A 2001 *J. Phys.: Condens. Matter* **13** 4105

[12] Hoppe U, Brow R K, Ilieva D, Jóvári P and Hannon A C 2005 *J. Non.-Cryst. Solids* **351** 3179

[13] Hoppe U, Metwalli E, Brow R K and Neuefeind J 2002 *J. Non-Cryst. Solids* **297** 263

[14] Hoppe U, Ebendorff-Heidepriem H, Neuefeind J and Bowron D T 2001 *Z. Naturforsch.* **56a** 237

[15] Hoppe U, Walter G, Carl G, Neuefeind J and Hannon A C 2005 *J. Non-Cryst. Solids* **351** 1020

[16] Brow R K 2000 *J. Non-Cryst. Solids* **263&264** 1 and references therein.

[17] Matuszewski J, Kropiwnicka J and Znamierowska T 1988 *J. Solid State Chem.* **75** 285

[18] Hong H Y P 1974 *Acta Crystallogr.* **30** 1857

[19] Faber T E and Ziman J M 1965 *Philos. Mag.* **11** 153

[20] Waasmaier D and Kirfel A 1995 *Acta Crystallogr. A* **51** 416

[21] Hoppe U 1996 *J. Non-Cryst. Solids* **195** 138

[22] Hoppe U, Walter G, Kranold R and Stachel D 2000 *J. Non-Cryst. Solids* **263-264** 29

[23] Clark E B, Mead R N and Mountjoy G 2006 *J. Phys.: Condens. Matter* **18** 6815

[24] Gaskell P H, Eckersley M C, Barnes A C and Chieux P 1991 *Nature* **350** 675

[25] Blétry J 1990 *Philos. Mag. B* **62** 469

[26] Hermann H, Elsner A and Stoyan D 2007 *J. Non-Cryst. Solids* **353** 3693

[27] Ilieva D, Kovacheva D, Cole J M and Gutzov I 2002 *Phosphorus Res. Bull.* **13** 137

Table 1

Weighting factors $(2-\delta_{ij})\, c_i\, b_i\, b_j\, / \langle b_i \rangle^2$ of pair distances in radial distribution functions calculated for the neutron (or X-ray) diffraction data of $R(PO_3)_3$ glasses: The area of a distance peak of atoms of sort j surrounding an atom of sort i with molar fraction c_i is related to the coordination number N_{ij} where the corresponding weighting factors are given in this table. The Kronecker symbol δ_{ij} is unity in case of $i=j$, otherwise zero. The scattering lengths b_i in case of neutron scattering are replaced by the electron numbers z_i in case of X-ray diffraction. (X-ray weighting factors depend on Q and, therefore, the peak areas depend on the conditions of the Fourier transformations. The weighting factors calculated by z_i are valid for $Q=0$ and give approximate values. The factors in this table are not identical with the $w_{ij}(Q)$ introduced in Chapter 3.

R atom	radiation	$ij = RR$	RP	RO	PP	PO	OO
La	X-ray	1.395	0.734	0.392	0.290	0.309	0.247
La	neutron	0.153	0.191	0.216	0.178	0.403	0.685
Yb	X-ray	1.822	0.781	0.416	0.251	0.268	0.214
Yb	neutron	0.312	0.259	0.292	0.160	0.363	0.615

Table 2

Minimum separation distances, Lm_{ij}, of pairs of atoms i and j as used in the RMC runs. The distances are given in nm.

R atom	$ij = RR$	RP	RO	PP	PO	OO
La	0.370	0.342	0.218	0.270	0.130	0.222
Nd	0.370	0.338	0.214	0.270	0.130	0.222
Er	0.370	0.338	0.210	0.270	0.130	0.222
Yb	0.370	0.334	0.206	0.270	0.130	0.222

Table 3

Coordination numbers (N_{RRm}) and mean distances (r_{RRm}) of the first peaks numbered by m which are identified in the pair distribution functions $g_{RR}(r)$ shown in Fig. 3. Lower and upper limits $r_{\max\, m-1}$ and $r_{\max\, m}$ for determination of the values N_{RRm} are estimated from the minima positions in the $g_{RR}(r)$ functions. Parameters N_{RO} and r_{RO} are taken from a previous paper [12]. All lengths are given in nm.

R atom	N_{RO}	r_{RO}	N_{RR1}	r_{RR1}	$r_{\max\,1}$	N_{RR2}	r_{RR2}	$r_{\max\,2}$	N_{RR3}	r_{RR3}	$r_{\max\,3}$
La	6.9±0.3	0.248±0.002	1.26±0.4	0.47±0.02	0.516	7.90±0.2	0.65±0.01	0.760	9.6±0.3	0.87±0.02	0.966
Nd	6.9±0.3	0.241±0.002	1.18±0.4	0.45±0.02	0.506	7.70±0.2	0.64±0.01	0.750	9.2±0.3	0.86±0.02	0.956
Er (Y)	6.5±0.3	0.226±0.002	0.78±0.3	0.43±0.02	0.484	7.14±0.2	0.62±0.01	0.726	8.9±0.3	0.84±0.02	0.930
Yb	6.5±0.3	0.225±0.002	0.38±0.3	0.44±0.02	0.482	7.10±0.2	0.61±0.01	0.716	8.8±0.3	0.83±0.02	0.920

Table 4

Illustration of the relations between the R–O coordination numbers, N_{RO}, the fractions of oxygen atoms (O$_{T,n}$, O$_{B,n}$) with different numbers n of R neighbours and the values N_{RRm} for the La(PO$_3$)$_3$ and Yb(PO$_3$)$_3$ crystals [17,18], a model (m7) of idealized behaviour with $N_{RO} = 7$ and the RMC models of the La(PO$_3$)$_3$ and Yb(PO$_3$)$_3$ glasses. Values N_{RO} given in parentheses were obtained from Gaussian fits [12].

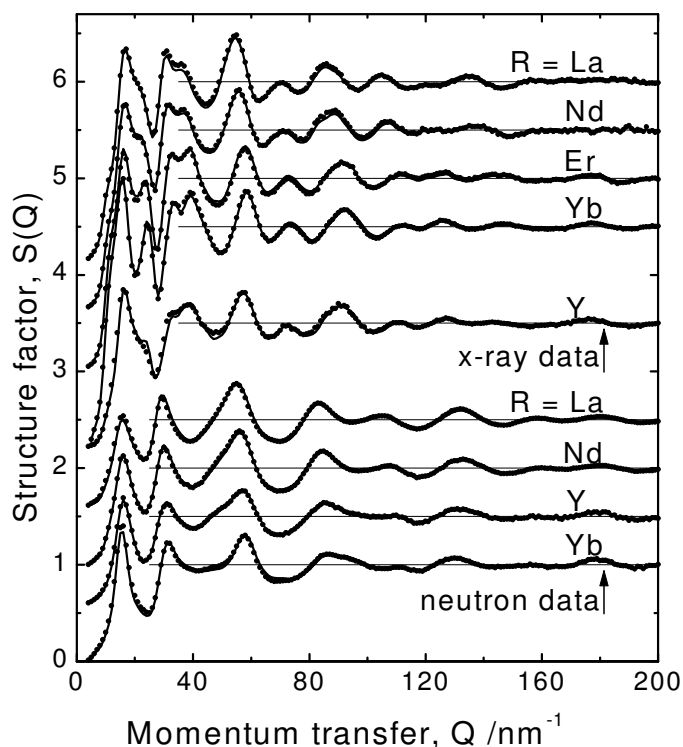| Sample	N_{RO}	O$_T$	O$_B$	O$_{T,0}$	O$_{T,1}$	O$_{T,2}$	O$_{B,0}$	O$_{B,1}$	N_{RR1}	N_{RR2}	N_{RR3}
c-La(PO$_3$)$_3$	8.0	0.666	0.333	0	0.444	0.222	0.333	0	2.0	12.0	6.0
m7-model	7.0	0.666	0.333	0	0.555	0.111	0.333	0	1.0	---	---
c-Yb(PO$_3$)$_3$	6.0	0.666	0.333	0	0.666	0	0.333	0	0	8.0	12.0
RMC-La(PO$_3$)$_3$	6.3 (6.9)	0.682	0.318	0.058	0.592	0.032	0.277	0.041	1.3	7.9	9.6
RMC-Yb(PO$_3$)$_3$	5.8 (6.5)	0.684	0.316	0.078	0.598	0.008	0.281	0.035	0.4	7.1	8.8

Fig. 1. Comparison of the experimental structure factors from X-ray and neutron diffraction of $R(PO_3)_3$ glasses [8,11-13] with those calculated from the resulting RMC configurations. The X-ray data of the Y(PO$_3$)$_3$ glass were not used in RMC but the corresponding $S_X(Q)$ factor is calculated from the RMC models obtained by neutron data of the Y(PO$_3$)$_3$ glass and X-ray data of the Er(PO$_3$)$_3$ glass. Both glasses, i.e., those with R = Y and Er, reveal to possess identical structures. The upper curves are shifted for clarity.
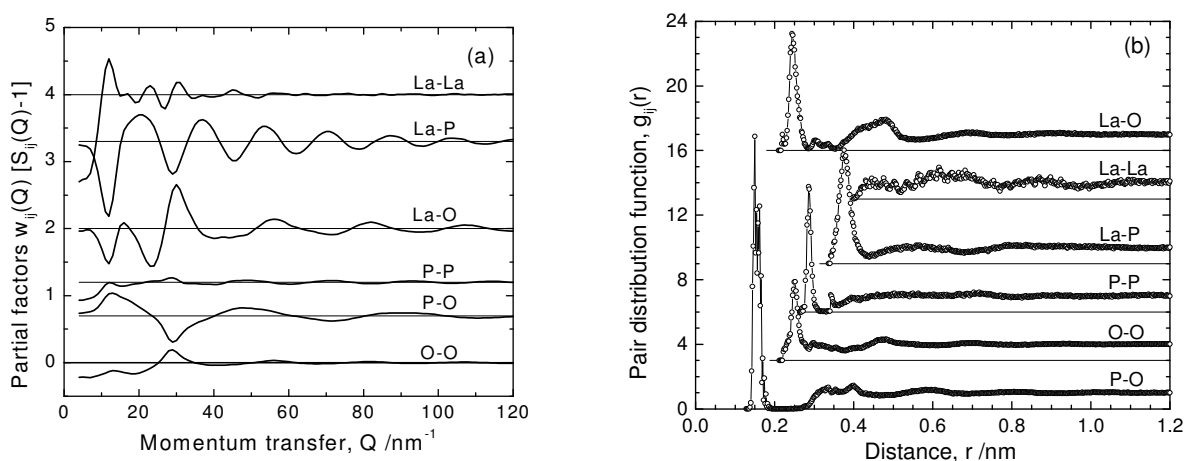
Fig. 2. Partial structure factors $S_{ij}(Q)$ multiplied with the X-ray weighting factors $w_{ij}(Q)$ (a) and the pair distribution functions $g_{ij}(r)$ (b) obtained by RMC for the La(PO$_3$)$_3$ glass. The upper curves are shifted for clarity.
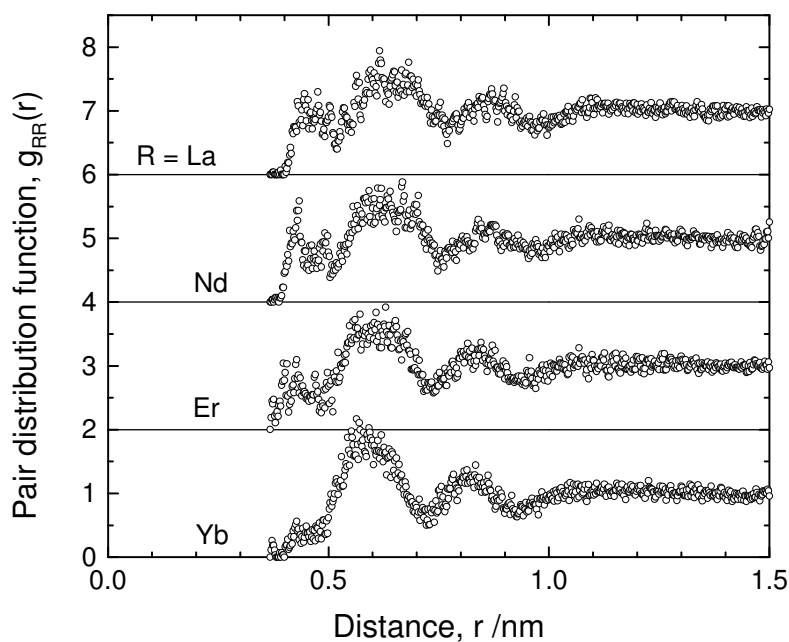
Fig. 3. R–R pair distribution functions $g_{RR}(r)$ obtained by RMC for the rare-earth metaphosphate glasses R(PO$_3$)$_3$ with R = La, Nd, Er(Y), Yb. The upper curves are shifted for clarity.
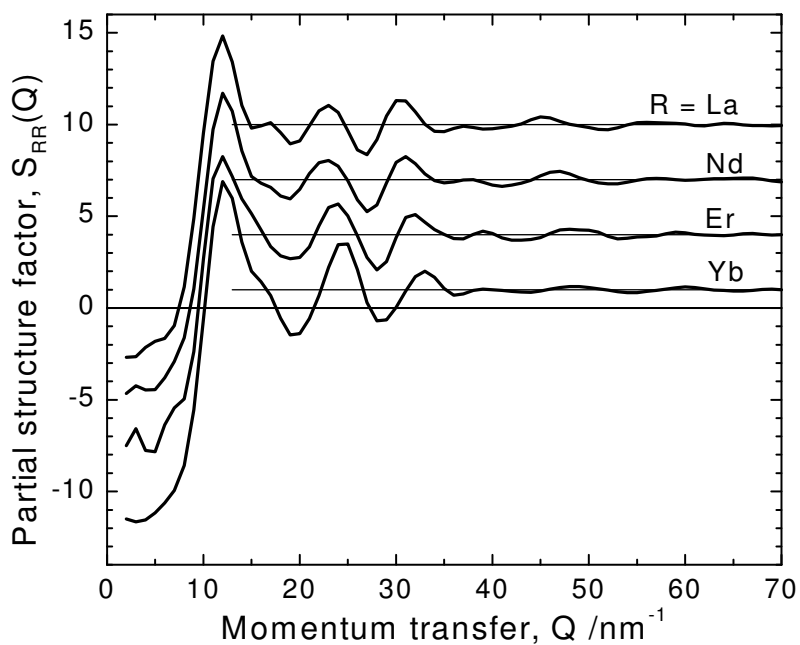

Fig. 4. R–R partial structure factors $S_{RR}(Q)$ which correspond to the $g_{RR}(r)$ functions shown in Fig. 3. The upper curves are shifted for clarity.
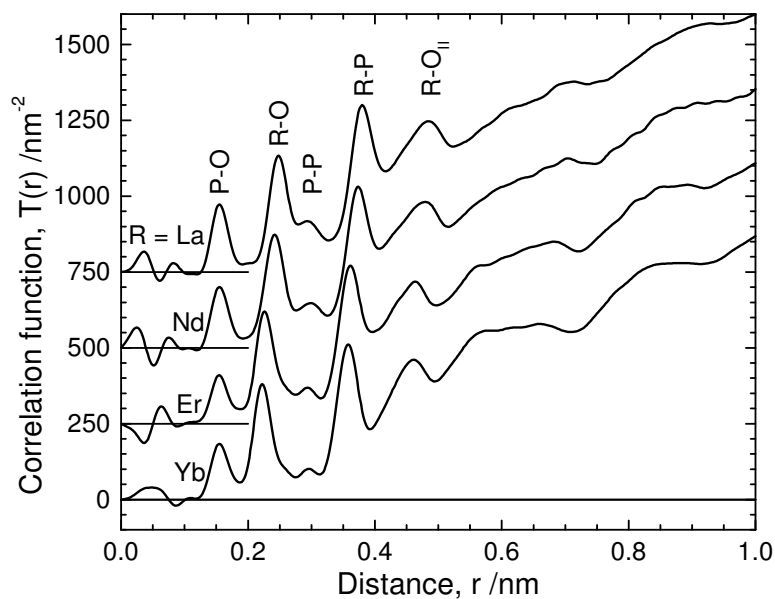
Fig. 5. Total correlation functions (X-rays) of the R(PO$_3$)$_3$ glasses studied [12]. P–O, R–O, O–O, P–P and R–P first-neighbour distances are clearly identified. The peak at ~0.48 nm is mainly attributed to R–O second neighbours. The broad peaks at ~0.65 and ~0.85 nm are assumed to be mainly due to R–R correlations.
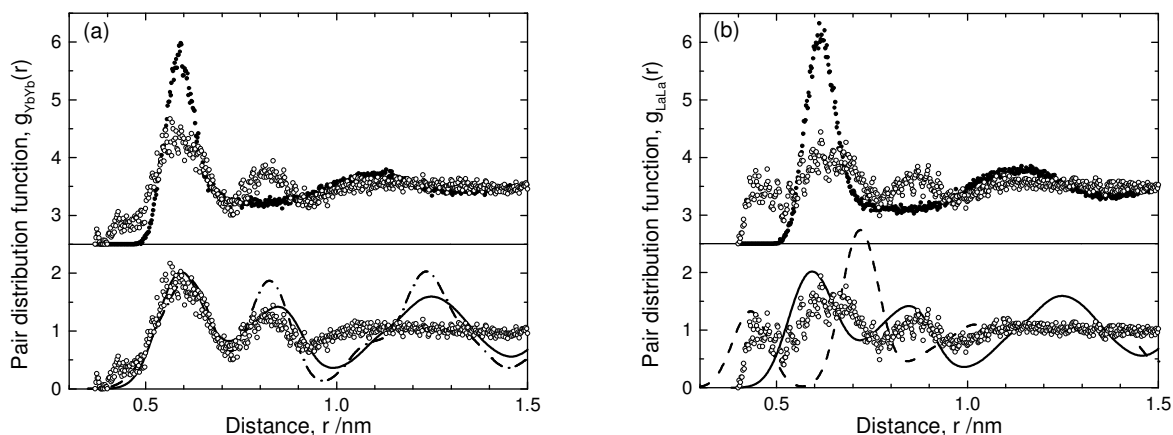

Fig. 6. Comparisons of the $g_{RR}(r)$ functions obtained from RMC for R(PO$_3$)$_3$ glasses with R = Yb (a) and La (b) with the $g_{RR}(r)$ functions calculated for a random packing of soft spheres and $g_{RR}(r)$ functions calculated from R–R distances of related crystal structures: monoclinic Yb(PO$_3$)$_3$ crystal [18] (solid lines), orthorhombic La(PO$_3$)$_3$ crystal [17] (dashed line), hexagonal order of Yb sites (dash-dotted line). Mean diameters of spheres of 0.58 and 0.61 nm and packing fractions of 0.54 and 0.62 are used for the model of random packing of R-centred spheres for R = Yb and La, respectively.